

# Variational Quantum Circuits for Quantum State Tomography

Yong Liu,<sup>1,\*</sup> Dongyang Wang,<sup>1,\*</sup> Shichuan Xue,<sup>1</sup> Anqi Huang,<sup>1</sup> Xiang Fu,<sup>1</sup> Xiaogang Qiang,<sup>1,2</sup>  
Ping Xu,<sup>1</sup> He-Liang Huang,<sup>3,4,5</sup> Mingtang Deng,<sup>1</sup> Chu Guo,<sup>6,†</sup> Xuejun Yang,<sup>1</sup> and Junjie Wu<sup>1,‡</sup>

<sup>1</sup>*Institute for Quantum Information & State Key Laboratory of High Performance Computing,  
College of Computer, National University of Defense Technology, Changsha 410073, China*

<sup>2</sup>*National Innovation Institute of Defense Technology, AMS, 100071 Beijing, China*

<sup>3</sup>*Henan Key Laboratory of Quantum Information and Cryptography, IEU, Zhengzhou 450001, China*

<sup>4</sup>*Hefei National Laboratory for Physical Sciences at Microscale and Department of Modern Physics,  
University of Science and Technology of China, Hefei, Anhui 230026, China*

<sup>5</sup>*CAS Centre for Excellence and Synergetic Innovation Centre in Quantum Information and Quantum Physics,  
University of Science and Technology of China, Hefei, Anhui 230026, China*

<sup>6</sup>*Quantum Intelligence Lab, Supremacy Future Technologies, Guangzhou 511340, China*

(Dated: May 2, 2022)

We propose a hybrid quantum-classical algorithm for quantum state tomography. Given an unknown quantum state, a quantum machine learning algorithm is used to maximize the fidelity between the output of a variational quantum circuit and this state. The number of parameters of the variational quantum circuit grows linearly with the number of qubits and the circuit depth. After that, a subsequent classical algorithm is used to reconstruct the unknown quantum state. We demonstrate our method by performing numerical simulations to reconstruct the ground state of a one-dimensional quantum spin chain, using a variational quantum circuit simulator. Our method is suitable for near-term quantum computing platforms, and could be used for relatively large-scale quantum state tomography for experimentally relevant quantum states.

## I. INTRODUCTION

Identifying a quantum state is a key step to verify or benchmark any quantum processes [1–4]. The quantum state tomography (QST) is a standard technology to fully identify an unknown quantum state, and is widely used in many quantum experiments [5–7]. Brute-force technique for QST however requires an exponential growing number of measurements, which could be feasible only for a very few number of qubits [8].

Various approaches has been used to alleviate this exponential scaling in the original proposal by assuming certain structural information about the target quantum state. An outstanding class of methods is based on tensor network states [9–11], which is known to be able to efficiently represent quantum states with bounded entanglement entropy through only a polynomial number of parameters. Thus for such quantum states only a polynomial number of measurements is required [12]. Other examples along this line include compressed sensing, which reduces the number of measurements with the assumption that the target quantum state is sparse [13, 14], and permutationally invariant tomography [15, 16].

Very recently, neural network models are also used to approximate and reconstruct quantum states. Unlike the above methods which made particular assumptions about the structure of the underlying quantum state, neural network based methods do not require prior informa-

tion about the state, but try to encode the information of the quantum state into the a parametric neural network based on the measurement outcomes. Such examples include restricted Boltzmann machine [17, 18], variational autoencoders [19], adaptive neural networks [20] and unsupervised generative models [21]. As a common feature of neural network based algorithms, for an unknown quantum state, it is unclear which class of the neural network could better capture the information of the quantum state. It is thus difficult to choose a universal structure of neural network which performs well for any quantum states.

In this work, we propose a hybrid quantum-classical method for quantum state tomography, as shown in Fig 1. In the quantum part, we apply quantum machine learning [22] to encode the information of the target quantum state into a variational quantum circuit, where the number of parameters scales polynomially with the number of qubits and the circuit depth. After that, a classical algorithm based on matrix product states (MPS) is used to reconstruct the quantum state. Unlike the tensor network states based methods, a variational quantum circuit is possible to approximate highly entangled quantum states with only a polynomial number of parameters [23, 24]. Compared to neural network based methods where the states are encoded within classical neural networks, our method is more natural in representing quantum states with parametric quantum circuits.

The content of this paper is organized as follows: In Sec. II, we show the quantum part of our algorithm, namely encoding the information of an unknown quantum state into a variational quantum circuit. In Sec. III, we show how to reconstruct the quantum state with matrix product states based on the determined parameters

\*These authors contribute equally to this work.

†Electronic address: guochu604b@gmail.com

‡Electronic address: junjiewu@nudt.edu.cn

of the variational quantum circuit. In Sec. IV, we demonstrate our method with numerical simulations by reconstructing the ground state of a quantum spin chain on a classical variational quantum circuit simulator. Finally, we conclude in Sec. V.

## II. APPROXIMATING QUANTUM STATE WITH VARIATIONAL QUANTUM CIRCUIT

The first step of our approach is to encode the information of the unknown quantum state into a variational quantum circuit, as shown in Fig. 1(a). The state under tomography is in general an  $n$ -qubit mixed state, which we denote as  $\hat{\rho}$ . To be able to fully capture the information in  $\hat{\rho}$ , we use a  $2n$ -qubit variational quantum circuit  $C_{2n}(\vec{\theta})$  (since it is enough to purify any  $n$ -qubit mixed state with  $n$  auxiliary qubits [25]), where  $\vec{\theta}$  contains all the parameters to be optimized. The output of the variational quantum circuit is denoted as  $|\psi^o\rangle$ , which is

$$|\psi^o\rangle = C_{2n}(\vec{\theta})|0\rangle^{\otimes 2n}. \quad (1)$$

We can then obtain the reduced density operator of the first  $n$  qubits by

$$\hat{\rho}^S = \text{tr}_A(|\psi^o\rangle\langle\psi^o|), \quad (2)$$

where  $\text{tr}_A$  means the partial trace over the latter  $n$  qubits. The fidelity between  $\hat{\rho}^S$  and  $\hat{\rho}$  can be represented by

$$\mathcal{F}(\vec{\theta}) = \text{tr}_S(\hat{\rho}\hat{\rho}^S) = \langle\psi^o|\hat{\rho}\otimes\hat{I}|\psi^o\rangle, \quad (3)$$

where  $\text{tr}_S$  means the trace over the former  $n$  qubits. Note that  $\mathcal{F}(\vec{\theta})$  can be efficiently computed with a quantum computer using SWAP test [26].

Our goal is then to maximize  $\mathcal{F}(\vec{\theta})$  over  $\vec{\theta}$ , for which we simply choose the loss function of our quantum machine learning algorithm as

$$f(\vec{\theta}) = 1 - \sqrt{\mathcal{F}(\vec{\theta})}. \quad (4)$$

If  $\hat{\rho}$  is known to be a pure state that can be written as  $\hat{\rho} = |\psi\rangle\langle\psi|$ , then only  $n$  qubits is required for our variational circuit. In this case,  $|\psi^o\rangle = C_n(\vec{\theta})|0\rangle^{\otimes n}$  and Eq.(4) can be simplified as

$$f(\vec{\theta}) = 1 - |\langle\psi^o|\psi\rangle|. \quad (5)$$

In Fig. 1(b) we show a possible implementation of the variational quantum circuit, which is consist of interlacing layers of rotation gates and two-qubit CNOT gates. To be able to represent generic quantum states, the rotational gates generally contain both parametric rotational X ( $R_x$ ) gates and rotational Y ( $R_y$ ) gates, which are defined as

$$R_x(\theta) = \begin{bmatrix} \cos \frac{\theta}{2} & -i \sin \frac{\theta}{2} \\ -i \sin \frac{\theta}{2} & \cos \frac{\theta}{2} \end{bmatrix}, \quad (6)$$

$$R_y(\theta) = \begin{bmatrix} \cos \frac{\theta}{2} & -\sin \frac{\theta}{2} \\ \sin \frac{\theta}{2} & \cos \frac{\theta}{2} \end{bmatrix}. \quad (7)$$

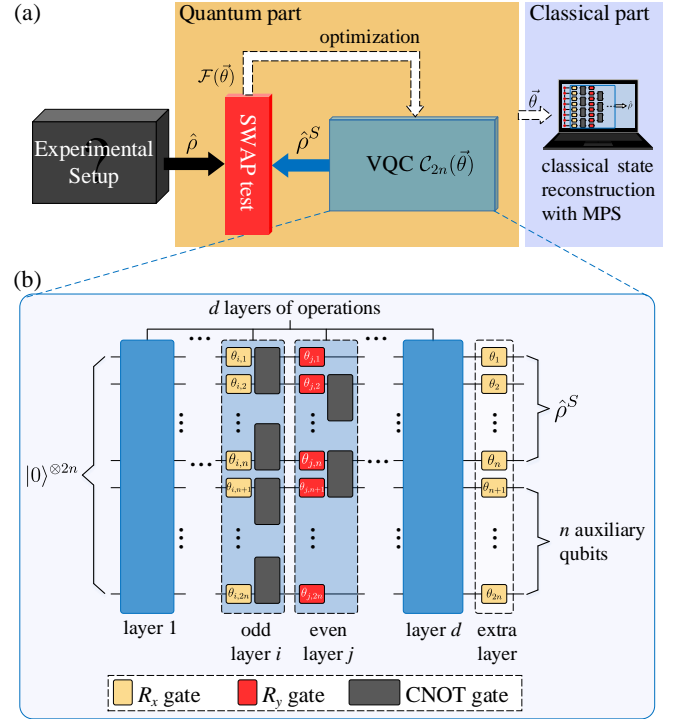


FIG. 1: (a) The scheme of the hybrid quantum-classical approach to quantum state tomography. The quantum part is to encode the information of the unknown state into a variational quantum circuit by maximizing the fidelity  $\mathcal{F}(\vec{\theta})$  measured through the SWAP test between the reduced density matrix of the first  $n$  qubits of the output state  $\hat{\rho}^S$  and the unknown state  $\hat{\rho}$ . Then a classical circuit simulator is used to reconstruct the state based on the determined parameters  $\vec{\theta}$  of the variational quantum circuit. (b) The scheme of the variational quantum circuit for state estimation. The circuit contains  $d$  layers of operations. The  $i^{\text{th}}$  layer contains  $2n$  single-qubit gates encoding the tunable parameters  $\{\theta_{i,1}, \theta_{i,2}, \dots, \theta_{i,2n}\}$ , and a group of commuting control-not (CNOT) gate operations applied on the neighbouring qubits alternately. The parametric single-qubit gates are respectively  $R_x$  gates in the odd layers or  $R_y$  gates in the even layers. The circuit ends up with an extra layer of single-qubit operations. The latter  $n$  auxiliary qubits are unnecessary if we have the prior knowledge that the unknown state is pure.

In this circuit, each layer of CNOT gates is counted as one depth. Thus for such a variational quantum circuit with depth  $d$ , the total number of parameters is  $2n(d+1)$  in general, or  $n(d+1)$  if we know  $\hat{\rho}$  is a pure state in advance, because we can use Eq.(5) instead of Eq.(4) to describe the target state of optimization of the variational circuit. We also note that the structure in Fig. 1(a) closely resembles random quantum circuits, which can generate statistic distributions that is very difficult for a classical computer to produce.

To iteratively update the parameters  $\vec{\theta}$  to minimize the loss function, a gradient-based optimization method

is usually preferred. Using the chain rule, we have

$$\frac{\partial f(\vec{\theta})}{\partial \theta_i} = \frac{f(\vec{\theta})}{\partial \mathcal{F}(\vec{\theta})} \cdot \frac{\partial \mathcal{F}(\vec{\theta})}{\partial \theta_i}. \quad (8)$$

The first term on the right hand side of Eq.(8) can be computed using a classical computer as long as we have obtained the output  $\mathcal{F}(\vec{\theta})$  from the quantum computer, and the second term on the right hand side of Eq.(8) can be computed using a quantum computer through [27]

$$\frac{\partial \mathcal{F}(\vec{\theta})}{\partial \theta_i} = \frac{1}{2} \mathcal{F}(\vec{\theta}_i^+) - \frac{1}{2} \mathcal{F}(\vec{\theta}_i^-), \quad (9)$$

where  $\vec{\theta}_i^\pm$  is the array of parameters obtained by adding or subtracting the  $i^{th}$  parameters of  $\vec{\theta}$  by  $\pi/2$ .

For one iteration of the algorithm, besides the evaluation of  $\mathcal{F}(\vec{\theta})$ , it is also required to evaluate  $\mathcal{F}(\vec{\theta}_i^\pm)$  for all  $2n(d+1)$  parameters to calculate the gradient. A single evaluation of  $\mathcal{F}(\vec{\theta})$  requires to execute the circuit for a constant number of times to reach a certain precision in the  $n$ -qubit SWAP test, and each execution involves around  $3nd$  gate operations. As a result, the complexity of one iteration is  $O(n^2 d^2)$ .

### III. STATE RECONSTRUCTION WITH MPS

The variational quantum circuit would store almost all the information of the unknown state as long as the above quantum machine learning algorithm managers to minimize the value of  $f(\vec{\theta})$  to close to 0, that is  $\hat{\rho}^S \approx \hat{\rho}$ . Then we can reconstruct the unknown state by simulating the evolution by the variational quantum circuit on a classical computer. Exactly simulating this process would require an exponential amount ( $O(2^{2n})$ ) of memory to store the full wavefunction as a state vector. In the following we show how to reconstruct  $\hat{\rho}^S$  with matrix product states [28]. The MPS representation of the  $2n$ -qubit state can be written as [29]

$$|\phi\rangle = \sum_{\sigma_1, \dots, \sigma_{2n}} \mathcal{G}(B^{\sigma_1} B^{\sigma_2} \dots B^{\sigma_{2n}}) |\sigma_1, \sigma_2, \dots, \sigma_{2n}\rangle. \quad (10)$$

Each  $B_{a_l, a_{l+1}}^{\sigma_l}$  is a rank-3 tensor, where  $\sigma_l$  represents the physical index and  $a_l$  represents the auxiliary index. Function  $\mathcal{G}$  means summation over common auxiliary indices. Here we also assume that the MPS is prepared in the *right canonical* form, namely  $B_{a_l, a_{l+1}}^{\sigma_l}$  satisfies

$$\sum_{\sigma_l, a_{l+1}} B_{a_l, a_{l+1}}^{\sigma_l} \text{conj}(B_{a'_l, a_{l+1}}^{\sigma_l}) = \delta_{a_l, a'_l}, \quad (11)$$

where  $\text{conj}(M)$  means to take the elementwise conjugate of the tensor  $M$ , and  $\delta_{i,j}$  is the Kronecker matrix satisfying  $\delta_{i,j} = 1$  for  $i = j$  and 0 otherwise. The maximum size

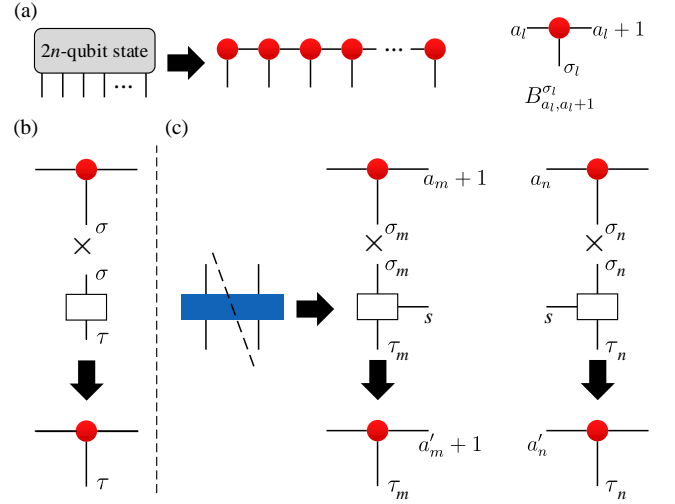


FIG. 2: Reconstructing the quantum state using a classical simulator based on matrix product states. (a) A  $2n$ -qubit quantum states represented with matrix product states. Each qubit is represented by a rank-3 tensor  $B_{a_l, a_{l+1}}^{\sigma_l}$ ; (b) Applying a single-qubit operation on a local tensor of MPS, which does not affect the sizes of the tensors; (c) A two-qubit gate operation is first decomposed into two local operations, and then applied to nearest-neighbour qubits respectively. The sizes of the tensors increase in general after this operation.

of the auxiliary indices is referred as the bond dimension  $\chi$ , namely

$$\chi = \max_{1 \leq l \leq 2n-1} \dim(a_l). \quad (12)$$

The initial state of the variational quantum circuit,  $|0\rangle^{\otimes 2n}$ , can be easily written as a separable MPS with  $\chi = 1$ , which is shown in Fig. 2(a). Then the single-qubit and two-qubit gates are applied to the MPS in a way that the right canonical form of the MPS is preserved. The single-qubit and two-qubit gate operations on MPS are shown in Fig. 2(b,c) respectively. For detailed mathematical description of these operations, one can refer to, for example [29, 30]. Note that each time a two-qubit gate is performed on a nearest neighbour pair of qubits, the bond dimension will effectively increase by a factor of  $\chi_o$ , which is the rank of the two-qubit operation. In case of a CNOT gate we have  $\chi_o = 2$  [31]. As a result, for a variational quantum circuit defined as in Fig. 1(a) with depth  $d$ , the final MPS will have a bond dimension

$$\chi \leq 2^{\frac{d}{2}}. \quad (13)$$

After the evolution, we trace out the latter  $n$  qubits for the resulting MPS and get the reduced density matrix as a matrix product operator (MPO)

$$\hat{\rho}^S = \sum_{\sigma_1, \dots, \sigma_n, \sigma'_1, \dots, \sigma'_n} \mathcal{G}(B^{\sigma_1} \dots B^{\sigma_n} B^{\sigma'_1} \dots B^{\sigma'_n}) |\sigma_1, \dots, \sigma_n\rangle \langle \sigma'_1, \dots, \sigma'_n|, \quad (14)$$

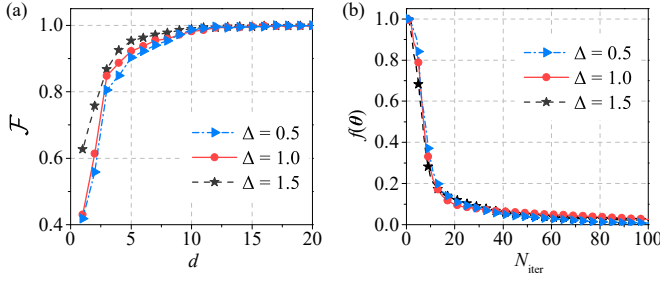


FIG. 3: (a) Final fidelity as a function of the depth of the circuit. (b) Loss values as a function of the number of iterations given  $d = 20$ . The ‘unknown’ quantum state is chosen to be the ground state of a one-dimension XXZ chain of 15 spins (qubits). In both the figures, the blue dashed-dot line with triangle, the red line with circle and the black dashed line with star correspond to  $\Delta = 0.5, 1, 1.5$  respectively.

with

$$\begin{aligned} & \mathcal{G} \left( B^{\sigma_1} \dots B^{\sigma_n} B^{\sigma'_1} \dots B^{\sigma'_n} \right) \\ &= \sum_{\substack{a_1, \dots, a_n, a_{n+1} \\ a'_1, \dots, a'_n, a'_{n+1}}} B_{a_1, a_2}^{\sigma_1} \dots B_{a_n, a_{n+1}}^{\sigma_n} B_{a'_1, a'_2}^{\sigma'_1} \dots B_{a'_n, a'_{n+1}}^{\sigma'_n}, \end{aligned} \quad (15)$$

where we have exploited the property of the MPS shown in Eq.(11). Finally, the MPO shown in Eq.(14) contains all the information of  $\hat{\rho}^S$ , whose size is bounded by  $4n\chi^2 = 4n2^d$ , and the component of  $\hat{\rho}^S$  in a particular basis  $|\tau_1, \dots, \tau_n\rangle \langle \tau'_1, \dots, \tau'_n|$  can be computed by

$$\langle \tau'_1, \dots, \tau'_n | \hat{\rho}^S | \tau_1, \dots, \tau_n \rangle = \mathcal{G} \left( B^{\tau_1} \dots B^{\tau_n} B^{\tau'_1} \dots B^{\tau'_n} \right), \quad (16)$$

where the computational complexity is  $O(\chi^3)$ .

#### IV. NUMERICAL SIMULATION AND PERFORMANCE ANALYSIS

To demonstrate our method, we implemented numerical simulations based on a variational quantum circuit simulator [32, 33]. Although our method can be used to approximate density operators in general, here we consider the case that the target state is a unitary state. Moreover, it is the ground state of a local spin Hamiltonian, the Heisenberg XXZ spin chain

$$\begin{aligned} \hat{H}_{XXZ} = & \sum_{l=1}^{L-1} [J (\hat{\sigma}_l^x \hat{\sigma}_{l+1}^x + \hat{\sigma}_l^y \hat{\sigma}_{l+1}^y) + \Delta \hat{\sigma}_l^z \hat{\sigma}_{l+1}^z] \\ & + h \sum_{l=1}^L \hat{\sigma}_l^z, \end{aligned} \quad (17)$$

where  $L$  is the number of spins (qubits),  $h$  is the magnetization strength,  $J$  is the tunneling strength, and  $\Delta$  is

the interaction strength. We fix  $L = 15$ ,  $h = 1$ ,  $J = 1$  in our simulations and the ground state is a function of  $\Delta$ , which we denote as  $|GS(\Delta)\rangle$ .  $\hat{H}_{XXZ}$  is gapless when  $\Delta \leq 1$  and gapped when  $\Delta > 1$ . We then use a variational quantum circuit to approximate  $|GS(\Delta)\rangle$ , which contains  $2^{15} \approx 3.2 \times 10^4$  parameters if stored as a state vector. Based on the priori knowledge that the ‘unknown’ quantum state is a pure state, we could simply use the loss function defined in Eq.(5). Moreover, since  $|GS(\Delta)\rangle$  contains only real numbers, we only use parametric  $R_y$  gates in our variational quantum circuits. We tune our variational quantum circuits with different depths to approximate the target state  $|GS(\Delta)\rangle$ , and the result is shown in Fig. 3.

In Fig. 3(a), we plot the final fidelity between the output of the variational quantum circuits and  $|GS(\Delta)\rangle$  as a function of the depth  $d$  for  $\Delta = 0.5, 1$  and  $1.5$  respectively. We can see that with only a few number of parameters, the state  $|GS(\Delta)\rangle$  can be approximated with a very high precision. More concretely, with a circuit depth of  $d = 15$  (240 parameters), we could reach a fidelity of above 99.1% for all the three cases. Also we notice that for larger value of  $\Delta$ , we need fewer number of parameters to reach a similar precision. This meets the expected since in that case the entanglement of the system is bounded and can even be efficiently simulated classically [34, 35]. In Fig. 3(b) we plot the loss function against the number of iterations. In particular, we find a precision of  $f(\vec{\theta}) \leq 0.05$  could be reached with  $N_{\text{iter}} = 50, 44, 34$  and a precision of  $f(\vec{\theta}) \leq 0.01$  could be reached with  $N_{\text{iter}} = 240, 209, 206$ , for  $\Delta = 0.5, 1, 1.5$  respectively.

#### V. CONCLUSION

In this work, we proposed a hybrid quantum-classical method for quantum state tomography. The quantum part of our method utilize quantum machine learning to encode the information of the unknown quantum state into a variational quantum circuit, which requires only a polynomial number of gate operations for a quantum computer and hopefully can be executed on near-term quantum computers. Then based on the parameters of the variational quantum circuit, we use matrix product states to reconstruct the unknown quantum state on a classical computer. The final density matrix will be stored as a matrix product operator. The classical complexity in both time and space within this step will in general grow exponentially with the circuit depth, but only linearly with the number of qubits. It’s also worth noting that our method is equally applicable to both pure states and mixed states. To demonstrate our method, we apply it to approximate and then reconstruct a 15-qubit ground state of a local spin Hamiltonian based on a variational quantum circuit simulator and show that a high fidelity could be reached with a relatively small number of variational parameters and iterations.



## Acknowledgments

The numerical simulation is done by the open source variational quantum circuit simulator VQC [36]. We gratefully acknowledge the help from China Greatwall Technology in Changsha. We appreciate the helpful discussion with other members of QUANTA group. J. W. acknowledges the support from the National Natural Science Foundation of China under Grant 61632021. C. G. acknowledges the support from the National Natural Science Foundation of China under Grants No. 11504430

and No. 11805279. P. X. acknowledges support from National Natural Science Foundation of China under Grants No. 11621091 and No. 11690031. X. Q. acknowledges support from National Natural Science Foundation of China under Grants No. 11804389. H.-L. H. acknowledges support from the Open Research Fund from State Key Laboratory of High Performance Computing of China (Grant No. 201901-01), National Natural Science Foundation of China under Grant No. 11905294, and China Postdoctoral Science Foundation.

- 
- [1] D. T. Smithey, M. Beck, M. G. Raymer, and A. Faridani, *Phys. Rev. Lett.* **70**, 1244 (1993).
  - [2] K. Vogel and H. Risken, *Phys. Rev. A* **40**, 2847 (1989).
  - [3] U. Leonhardt, *Phys. Rev. Lett.* **74**, 4101 (1995).
  - [4] T. J. Dunn, I. A. Walmsley, and S. Mukamel, *Phys. Rev. Lett.* **74**, 884 (1995).
  - [5] C.-Y. Lu, X.-Q. Zhou, O. Gühne, W.-B. Gao, J. Zhang, Z.-S. Yuan, A. Goebel, T. Yang, and J.-W. Pan, *Nature Physics* **3**, 91 (2007).
  - [6] H. Häffner, W. Hänsel, C. F. Roos, J. Benhelm, D. Chekhal kar, M. Chwalla, T. Körber, U. D. Rapol, M. Riebe, P. O. Schmidt, C. Becher, O. Gühne, W. Dür, and R. Blatt, *Nature* **438**, 643 (2005).
  - [7] D. F. V. James, P. G. Kwiat, W. J. Munro, and A. G. White, *Phys. Rev. A* **64**, 052312 (2001).
  - [8] A. G. White, D. F. V. James, P. H. Eberhard, and P. G. Kwiat, *Phys. Rev. Lett.* **83**, 3103 (1999).
  - [9] M. Cramer, M. B. Plenio, S. T. Flammia, R. Somma, D. Gross, S. D. Bartlett, O. Landon-Cardinal, D. Poulin, and Y.-K. Liu, *Nature Communications* **1**, 149 (2010).
  - [10] Y.-Y. Zhao, Z. Hou, G.-Y. Xiang, Y.-J. Han, C.-F. Li, and G.-C. Guo, *Opt. Express* **25**, 9010 (2017).
  - [11] J. Wang, Z.-Y. Han, S.-B. Wang, Z. Li, L.-Z. Mu, H. Fan, and L. Wang, *arXiv preprint arXiv:1712.03213* (2017).
  - [12] B. P. Lanyon, C. Maier, M. Holzäpfel, T. Baumgratz, C. Hempel, P. Jurcevic, I. Dhand, A. S. Buyskikh, A. J. Daley, M. Cramer, M. B. Plenio, R. Blatt, and C. F. Roos, *Nature Physics* **13**, 1158 (2017).
  - [13] D. Gross, Y.-K. Liu, S. T. Flammia, S. Becker, and J. Eisert, *Phys. Rev. Lett.* **105**, 150401 (2010).
  - [14] W.-T. Liu, T. Zhang, J.-Y. Liu, P.-X. Chen, and J.-M. Yuan, *Phys. Rev. Lett.* **108**, 170403 (2012).
  - [15] G. Tóth, W. Wieczorek, D. Gross, R. Krischek, C. Schwemmer, and H. Weinfurter, *Phys. Rev. Lett.* **105**, 250403 (2010).
  - [16] T. Moroder, P. Hyllus, G. Tóth, C. Schwemmer, A. Niggebaum, S. Gaile, O. Ghne, and H. Weinfurter, *New Journal of Physics* **14**, 105001 (2012).
  - [17] G. Torlai, G. Mazzola, J. Carrasquilla, M. Troyer, R. Melko, and G. Carleo, *Nature Physics* **14**, 447 (2018).
  - [18] G. Torlai and R. G. Melko, *Phys. Rev. Lett.* **120**, 240503 (2018).
  - [19] A. Rocchetto, E. Grant, S. Strelchuk, G. Carleo, and S. Severini, *npj Quantum Information* **4**, 28 (2018).
  - [20] Y. Quek, S. Fort, and H. K. Ng, *arXiv preprint arXiv:1812.06693* (2018).
  - [21] J. Carrasquilla, G. Torlai, R. G. Melko, and L. Aolita, *Nature Machine Intelligence* **1**, 155 (2019).
  - [22] J. Biamonte, P. Wittek, N. Pancotti, P. Rebentrost, N. Wiebe, and S. Lloyd, *Nature* **549**, 195 (2017).
  - [23] S. Boixo, S. V. Isakov, V. N. Smelyanskiy, R. Babbush, N. Ding, Z. Jiang, M. J. Bremner, J. M. Martinis, and H. Neven, *Nature Physics* **14**, 595 (2018).
  - [24] F. Arute, K. Arya, R. Babbush, D. Bacon, J. C. Bardin, R. Barends, R. Biswas, S. Boixo, F. G. S. L. Brandao, D. A. Buell, B. Burkett, Y. Chen, Z. Chen, B. Chiaro, R. Collins, W. Courtney, A. Dunsworth, E. Farhi, B. Foxen, A. Fowler, C. Gidney, M. Giustina, R. Graff, K. Guerin, S. Habegger, M. P. Harrigan, M. J. Hartmann, A. Ho, M. Hoffmann, T. Huang, T. S. Humble, S. V. Isakov, E. Jeffrey, Z. Jiang, D. Kafri, K. Kechedzhi, J. Kelly, P. V. Klimov, S. Knysh, A. Korotkov, F. Kostritsa, D. Landhuis, M. Lindmark, E. Lucero, D. Lyakh, S. Mandrà, J. R. McClean, M. McEwen, A. Megrant, X. Mi, K. Michielsen, M. Mohseni, J. Mutus, O. Naaman, M. Neeley, C. Neill, M. Y. Niu, E. Ostby, A. Petukhov, J. C. Platt, C. Quintana, E. G. Rieffel, P. Roushan, N. C. Rubin, D. Sank, K. J. Satzinger, V. Smelyanskiy, K. J. Sung, M. D. Trevithick, A. Vainsencher, B. Villalonga, T. White, Z. J. Yao, P. Yeh, A. Zalcman, H. Neven, and J. M. Martinis, *Nature* **574**, 505 (2019).
  - [25] Y. Ping, H. Li, X. Pan, M. Luo, and Z. Zhang, *International Journal of Theoretical Physics* **52**, 4367 (2013).
  - [26] H. Buhrman, R. Cleve, J. Watrous, and R. de Wolf, *Phys. Rev. Lett.* **87**, 167902 (2001).
  - [27] K. Mitarai, M. Negoro, M. Kitagawa, and K. Fujii, *arXiv preprint arXiv:1803.00745v3* (2018).
  - [28] A. McCaskey, E. Dumitrescu, M. Chen, D. Lyakh, and T. Humble, *PLOS ONE* **13**, 1 (2018).
  - [29] U. Schollwck, *Annals of Physics* **326**, 96 (2011), january 2011 Special Issue.
  - [30] H.-L. Huang, W.-S. Bao, and C. Guo, *Phys. Rev. A* **100**, 032305 (2019).
  - [31] C. Guo, Y. Liu, M. Xiong, S. Xue, X. Fu, A. Huang, X. Qiang, P. Xu, J. Liu, S. Zheng, H.-L. Huang, M. Deng, D. Poletti, W.-S. Bao, and J. Wu, *Phys. Rev. Lett.* **123**, 190501 (2019).
  - [32] E. Farhi and H. Neven, *arXiv preprint arXiv:1802.06002v2* (2018).
  - [33] A. Kandala, A. Mezzacapo, K. Temme, M. Takita, M. Brink, J. M. Chow, and J. M. Gambetta, *Nature* **549**, 242 (2017).
  - [34] M. B. Hastings, *Phys. Rev. B* **73**, 085115 (2006).

- [35] Z. Landau, U. Vazirani, and T. Vidick, [Nature Physics](#) **11**, 566 (2015).
- [36] Available on GitHub at <https://github.com/supremacyfuture/VQC>.